Chemical Geology 444 (2016) 110–119

Contents lists available at ScienceDirect

Chemical Geology

journal homepage: www.elsevier.com/locate/chemgeo

Fe(II)-induced phase transformation of ferrihydrite: The inhibition effects and stabilization of divalent metal cations

Chengshuai Liu [a,c], Zhenke Zhu [b], Fangbai Li [a,*], Tongxu Liu [a], Changzhong Liao [a,d], Jey-Jau Lee [e], Kaimin Shih [d], Liang Tao [a], Yundang Wu [a]

[a] Guangdong Key Laboratory of Agricultural Environment Pollution Integrated Control, Guangdong Institute of Eco-Environmental and Soil Sciences, Guangzhou 510650, PR China
[b] Institute of Subtropical Agriculture, Chinese Academy of Sciences, Changsha 410125, PR China
[c] State Key Laboratory of Environmental Geochemistry, Institute of Geochemistry, Chinese Academy of Sciences, Guiyang 550081, PR China
[d] Department of Civil Engineering, The University of Hong Kong, Pokfulam Road, Hong Kong, PR China
[e] National Synchrotron Radiation Research Center (NSRRC), Hsinchu 30076, Taiwan

ARTICLE INFO

Article history:
Received 8 April 2016
Received in revised form 30 September 2016
Accepted 4 October 2016
Available online 6 October 2016

Keywords:
Soil iron cycle
Recrystallization
Metal stabilization
Binding ability
Cation effect

ABSTRACT

The Fe(II)-induced phase transformation of iron (hydr)oxides is an important process in the geochemical iron cycle and is one in which the coexisting metal cations inhibit the phase transformation rates. However, the underlying affecting mechanisms by metal cations and the critical property of metal cations that is responsible for the inhibition remain unclear. In this study, we focus on the cation effect of seven divalent cations (denoted as Me(II), including Mg(II), Ca(II), Ba(II), Mn(II), Co(II), Ni(II), and Zn(II)) and their influencing mechanisms on Fe(II)-catalyzed transformation processes of ferrihydrite. At initial reaction conditions (i.e. pH 6.5 and 2.0 mM Fe(II)), the binding ability (the affinity of cations for ferrihydrite surface) of Me(II) was found to affect the ferrihydrite transformation. Me(II) with higher binding abilities reduced the bound-Fe(II) amount on ferrihydrite and decreased the redox potentials of the Fe(II)-catalyzed system to inhibit the transformation rates of ferrihydrite. In addition to the inhibition effect, the Me(II) was partly stabilized in the formed secondary iron minerals. The binding abilities of Me(II) also affected the Fe(II)-induced transformation pathways of ferrihydrite by affecting the amount of bound-Fe(II) on ferrihydrite. Ferrihydrite was first transformed to lepidocrocite and later to goethite and magnetite with Me(II) that had lower binding ability than Fe(II), whereas it was directly transformed to goethite and magnetite when with Me(II) that had higher binding ability than Fe(II).

1. Introduction

Iron minerals are one of the most active constituents of soils and play crucial roles in the biogeochemical cycles of soil elements (Borch et al., 2009). In addition to ferric reduction and ferrous oxidation, which were considered to be the general reaction steps of the iron cycle, the direct interplay between aqueous Fe(II) species and the structural Fe(III) in soil iron-bearing minerals is a more recently recognized reaction step in the iron cycle (Suter et al., 1988; Larese-Casanova and Scherer, 2007; Handler et al., 2014). The interplay mechanisms for electron transfer and Fe atom exchange between the aqueous Fe(II) and structural Fe(III) have emerged from the evidences provided by spectroscopic techniques and stable iron isotope tracers (Williams and Scherer, 2004; Pedersen et al., 2005; Handler et al., 2009; Neumann et al., 2015). One of the most notable observations is the accelerated phase transformation of iron (hydr)oxides, which leads to the formation of more stable iron (hydr)oxides, such as goethite, magnetite, and hematite (Hansel et al., 2005; Pedersen et al., 2005; Boland et al., 2014b). This process has implications for altering the bioavailability of the metallic contaminants, through being sequestered or released by the transformed iron (hydr)oxides (Pedersen et al., 2006; Nico et al., 2009; Frierdich et al., 2011; Frierdich and Catalano, 2012; Latta et al., 2012a).

Ferrihydrite is usually the first type of iron (hydr)oxide to be formed in the course of iron mineralization and is thermodynamically unstable compared with other crystalline iron (hydr)oxides (Cornell and Schwertmann, 2003; Jang et al., 2003). This thermodynamically unstable (hydr)oxide has been confirmed to be one of the easiest iron (hydr)oxides in recrystallization into lepidocrocite, goethite, and magnetite by aqueous Fe(II) species derived from either biotic or abiotic processes (Hansel et al., 2003, 2005; Boland et al., 2014b). In addition to the Fe(II)-accelerated transformation mechanisms, the environmental factors that affect the transformation rate and extent have also received attention. These factors, such as pH, temperature, O_2 concentration, and solution/solid-associated concentrations of Fe(II), can significantly influence the Fe(II)-induced transformation rates of ferrihydrite (Hansel et al., 2003, 2011; Das et al., 2011; Boland et al., 2013; Wang et al., 2013; Boland et al., 2014a, 2014b).

* Corresponding author.
E-mail address: cefbli@soil.gd.cn (F. Li).

http://dx.doi.org/10.1016/j.chemgeo.2016.10.002
0009-2541/

Metal cations are usually coexisted with or structurally incorporated in iron (hydr)oxides in soils, especially in polluted soils with metallic contaminants. Investigation of the effects of cations on the Fe(II)-induced transformation of iron (hydr)oxides, therefore, is of great importance for understanding the iron cycle, as well as the environmental geochemistry of soil metal contaminants (Borch et al., 2009; Frierdich et al., 2011). Many coexisting cations have been reported to affect the Fe(II)-induced transformation rates and pathways of ferrihydrite in previous studies (Jang et al., 2003; Jones et al., 2009; Das et al., 2011; Frierdich et al., 2011; Hansel et al., 2011; Latta et al., 2012b; Boland et al., 2014a). These previous studies also suggested possible influencing mechanisms, but they were not fully explored. The concentration of solid-associated Fe(II) on iron (hydr)oxides from aqueous Fe(II) is important in determining the reaction rates (Hansel et al., 2005; Burton et al., 2008; Reddy et al., 2015) and also affect the types of secondary minerals produced (Hansel et al., 2003, 2005; Boland et al., 2014b). Therefore, some studies have attributed the inhibition effects of cations to the competitive adsorption with Fe(II) and the consequently reduced reactive surface sites available to Fe(II) (Das et al., 2011; Hansel et al., 2011). Other studies, however, have indicated that the degree of Fe(II) uptake cannot fully explain the differences in the transformation rates of iron (hydr)oxides, including ferrihydrite (Latta et al., 2012b; Boland et al., 2014a, 2014b).

The physicochemical properties of metal cations are the essential factors that affect their behavior in reactions, such as the redox reactions, complexation, precipitation, and hydrolysis, as well as their affinities to iron (hydr)oxides (Rout et al., 2012; Dai and Hu, 2014). Environmental factors have been reported to affect the Fe(II)-induced reactions of iron (hydr)oxides (Hansel et al., 2005; Das et al., 2010; Boland et al., 2014b), especially the pH (Hansel et al., 2003, 2005) and Fe(II) concentrations (Massey et al., 2014b), which has been confirmed to be the important factors determining Fe(II)-induced ferrihydrite transformation kinetics and the end products. The intrinsic properties of metal cations, e.g., binding ability, ionic radii, etc., are also expected to affect the transformation processes of ferrihydrite with metal cations when at the constant environmental conditions. The presence of divalent metals is of particular interest during the Fe(II)-induced reaction of iron (hydr)oxides because they have the same valence state as Fe(II). For example, Mössbauer spectroscopy of Fe(II)-accelerated ferrihydrite transformation in the presence of some divalent cations, such as Zn(II), Cu(II), and Mn(II), indicated the formation of Fe(II)-deficient magnetite by the substitution of these divalent metals for structural Fe(II), due to the similarity in ionic radius to that of Fe(II) (Jang et al., 2003). One recent study found that an increase in Fe(II) concentration at and beyond the monolayer on/in hematite could conceivably inhibit atom exchange because the increase led to conditions that neutralized the surface potential gradient (Frierdich et al., 2015). The surface-layer Fe(II) on iron (hydr)oxides would result in electron transfer from Fe(II) to structural Fe(III) and then electron bulk conduction in iron (hydr)oxides (Yanina and Rosso, 2008). The divalent cations do not transfer electrons to structural Fe(III), however, the additional divalent cations would result in much higher monolayer condition of surface-layer cations. Additionally, the divalent cations would decrease the contacted Fe(II) of iron (hydr)oxides and neutralize the surface potential gradient. With less Fe(II) transferring electrons to the structural Fe(III) in iron (hydr)oxides, the electron bulk conduction in the solids would be decreased (Larese-Casanova and Scherer, 2007), and consequently, the Fe(II)-induced reaction of iron (hydr)oxides would be inhibited (Yanina and Rosso, 2008).

However, the effects on the Fe(II)-induced transformation of iron (hydr)oxides due to the properties of metal cations have not been well explored. Additionally, few studies on the geochemical processes of metals in iron minerals have focused on the environmental behavior of metal cations with the same valence state as Fe(II) during the Fe(II)-induced transformation of iron (hydr)oxides.

In this study, we focused on the cation effect of divalent metal ions on the phase transformation processes of ferrihydrite when reacted with fixed initial concentration of Fe(II), as well as the stabilization of metals in the formed secondary iron (hydr)oxides during the phase transformation. In the experiments, seven divalent metal ions, including Ba^{2+}, Ca^{2+}, Mg^{2+}, Mn^{2+}, Co^{2+}, Ni^{2+}, and Zn^{2+}, were used with the same fixed initial concentration at the buffered constant pH condition to explore the mechanisms of cation effect. In particular, we further investigated the physicochemical properties of metals correlated with the phase transformation rates of ferrihydrite and metal stabilization. Throughout, we centered on the fate of metal ions and transformation rates of ferrihydrite during the Fe(II)-induced reactions when coexisting with divalent metals. The aim was to define the roles of the basic intrinsic physicochemical properties of metal cations within this environmentally important reaction.

2. Materials and methods

2.1. Ferrihydrite preparation

Ferrihydrite was synthesized according to previously reported methods (Das et al., 2010; Boland et al., 2014b). Briefly, ferrihydrite was prepared by dissolving 20 g of $Fe(NO_3)_3 \cdot 9H_2O$ in 250 mL of double distilled deionized (DI) water and then titrated with 1 M KOH to pH 7–8. The resulting suspension was then centrifuged and subsequently washed with DDI water until the pH of the slurry approached the pH_{pzc} (~pH 7.5) of ferrihydrite. This stock suspension of ferrihydrite was refrigerated and used within three days. Some of the obtained ferrihydrite suspension was freeze-dried to confirm the phase by X-ray diffraction (XRD).

2.2. Experiments on Fe(II)-induced transformation of ferrihydrite

All transformation experiments were carried out inside an anoxic chamber (Model Bactron II, Anaerobic Chamber, 200 plate capacity, Shellab, Shedon Manufacturing, Inc., Cornelius, OR, US) to maintain anaerobic conditions. All solutions were purged with high purity N_2 for at least 2 h to remove oxygen before being transferred into the chamber and were then exposed to the anoxic chamber atmosphere for 48 h. A stock solution of 100 mM Fe(II) was prepared inside the anoxic chamber by dissolving $FeCl_2 \cdot 4H_2O$ in deoxygenated water. The 100 mM stock solutions of each of the studied metal cations (denoted by Me(II) in this paper), i.e., Mg(II), Ca(II), Ba(II), Mn(II), Co(II), Ni(II), and Zn(II), were all obtained by dissolving their respective chloride salts in deoxygenated water in the anoxic chamber. Each reactor contained 30 mM ferrihydrite (~3.2 g/L), 0 or 2.0 mM initial Fe(II), and 0 or 1.0 mM Me(II). The reaction pH 6.5 was used here in an attempt to simultaneously model typical soil conditions (Liu et al., 2014a) and obtain the condition of as high efficiency as possible in Fe(II)-induced reaction of iron (hydr)oxides (Reddy et al., 2015), which was buffered by 20 mM 1,4-piperazinediethanesulfonic acid (PIPES) with 20 mM KBr as a background electrolyte. The reagents were added following the order of ferrihydrite, buffer solution, and cation solution (equilibrating for 30 min), and then adding the Fe(II) solution to initiate the reactions. Serum bottles of 100 mL were used as the experimental reactors and were sealed with Teflon-coated butyl rubber stoppers and crimp seals after all of the target reagents were added. Finally, all of the reactors were wrapped in Al-foil and placed on an end-over-end rotator. Three triplicate reactors were sacrificed to be sampled for analyses at time intervals of 0.5, 1, 2, 4, 8, 15, 30, and 60 days.

2.3. Analyses of Fe(II) and Me(II)

After being sampled, two 5 mL aliquots were taken from each reactor suspension and placed into 10 mL centrifuge tubes. After being sealed with an O-ring Teflon tape and then covered tightly, the tubes

were centrifuged outside the anoxic chamber at 4500 rpm for 10 min and then immediately returned to the chamber. The supernatant was filtered through 0.22 μm nylon filters (Millipore, Boston, MA, USA) and acidified with 20 μL concentrated HCl. And then, the acidified solution was transferred out of the anoxic chamber to analyze the dissolved Fe(II) and Me(II). The solids from the two aliquots in the centrifuge tubes were added to 0.4 M HCl and concentrated HCl to be extracted and digested for 1.5 h and 0.5 h, respectively. After being centrifuged once again, the filtrated supernatant from the centrifuged 0.4 M HCl-extracted solution was used to analyze the 0.4 M HCl-extracted Fe(II), and the filtrated solution from the dissolution by concentrated HCl was used to analyze the stabilized Fe(II) and Me(II) in the solids (Reddy et al., 2015). The concentrations of the aqueous Fe(II) were determined by the Fe(II)-selective reagent ferrozine (Fadrus and Malý, 1975). The concentrations of the seven heavy metals were determined by inductively coupled plasma-optical emission spectroscopy (ICP-OES, Perkin-Elmer optima 2000, USA).

2.4. Characterization of the solid phase

The solids separated from the centrifugation described above were washed with DDI water followed by further centrifugation and then freeze-dried for characterization. The X-ray diffraction (XRD) patterns for phase identification and quantification were recorded on a D8 Advanced Diffractometer (Bruker AXS) and the BL17A1 beamline of the National Synchrotron Radiation Research Center (NSRRC) TLS light source in Taiwan. The ring energy of the TLS was operated at 1.5 GeV with a typical current of 360 mA. The wavelength of the incident X-rays was 1.321863 Å (~9.3 keV), delivered from the superconducting wavelength-shifting magnet and a Si(111) Triangular Crystal Monochromator. The diffraction patterns were recorded using a Mar345 imaging plate detector approximately 180 mm away from sample positions and with typical exposure duration of 5 min. The pixel size of Mar345 was 100 μm. The diffraction angles were calibrated according to the Bragg positions of LaB_6 standards. The two-dimensional diffraction pattern was converted to a one-dimensional powder diffraction profile using the program GSAS-II (Toby and Von Dreele, 2013) and cake-type integration. The powder sample was rotated quickly at approximately 300 rpm to avoid a preferred orientation. The phase identification was executed by matching the obtained XRD patterns with the pattern retrieved from the standard powder diffraction database of the International Centre for Diffraction Data (ICDD PDF-2, Release 2008) (Lu et al., 2013). Ferrihydrite is usually nanocrystalline with the ideal structure form containing 20% tetrahedrally and 80% octahedrally coordinated iron (Michel et al., 2007). As ferrihydrite is in poor crystalline, it was considered as amorphous contents in our quantitative analysis. To quantify both crystalline and poorly-crystalline phases, all the samples were mixed with 20 wt% of CaF_2 (449717-25G, Merck, Germany) as the standard reference in the Rietveld quantitative analysis carried out in the TOPAS program. The accuracy of this method has been discussed hugely and applied in many areas (De La Torre et al., 2001; Bernasconi et al., 2014).

The morphologies and crystallite sizes of the reacted solid samples were observed by transmission electron microscopy (TEM). For comparison, γ-FeOOH, α-FeOOH, and Fe_3O_4 were characterized directly after being prepared with methods reported previously (Cornell and Schwertmann, 2003) First, the solid samples were dispersed in absolute ethanol (≥99.5%) for ultrasonic shaking, and then deposited on holey-carbon film Cu grids. The images were then recorded on a Philips-CM12 TEM operated at 200 kV with the dried grids.

Electrochemical measurements were used to probe the influence of additional Me(II) on the redox process of the Fe(II) on the ferrihydrite surface. The measurements were performed at room temperature in a conventional three-electrode cell connected to an electrochemical workstation (CHI660D, Shanghai Chenhua Instruments Co., China). A glassy carbon (GC) electrode (3.0 mm in diameter) coated with ferrihydrite was used as the working electrode. A saturated calomel electrode (SCE) and a Pt plate were used as the reference and counter electrodes, respectively. Cyclic voltammograms (CVs) were performed in an N_2-saturated 2 mM Fe(II) solution amended with1 mM of the various Me(II) at room temperature at a scan rate of 50 mV/s.

3. Results

3.1. The effects of metal cations on Fe(II)-induced phase transformation rates and pathways of ferrihydrite

To investigate the effects of different Me(II) on the phase transformation of ferrihydrite, we carried out the anaerobic batch experiments for the Fe(II)-induced reactions of ferrihydrite in the presence of different Me(II) at controlled pH 6.5. The phase constituents of the solids during the transformation processes of ferrihydrite were identified with XRD (Fig. 1), and the results quantitatively showed the different processes of Fe(II)-induced transformation of ferrihydrite in the presence of different Me(II). As indicated by the XRD patterns in Fig. 1, the compositions of the secondary formed minerals were different in the presence of different Me(II), and different Fe(II)-transformation pathways of ferrihydrite were obtained. In the treatment without Me(II) (Control), ferrihydrite was transformed by Fe(II) quickly and disappeared completely within 4 days, induced from the diffraction patterns of the XRD characterization results. The relative diffraction peak intensities of lepidocrocite increased quickly for 2 days and then decreased due to the gradual Fe(II)-induced transformation to goethite and magnetite (Fig. 1A). The presence of the alkaline earth metal cations, Mg(II), Ca(II), and Ba(II), did not change the pathway of the ferrihydrite phase transformation compared with the control treatment. More interesting results were obtained with the transition metal cations. With the transition metal cation Mn(II), ferrihydrite was also transformed to lepidocrocite first, but the further transformations to goethite and magnetite were not completed until approximately 8 days and 30 days, respectively. This observation indicated the inhibition of Mn(II) on the Fe(II)-induced phase transformation for both ferrihydrite and the formed lepidocrocite. The other three transition metals, Co(II), Ni(II), and Zn(II), induced a different pathway for the phase transformation of ferrihydrite. During the transformation, no representative peaks of lepidocrocite were detected in the XRD patterns even over the short time interval of 0.5 day (Fig. 1D, F, and H), showing that the ferrihydrite was directly transformed into goethite and magnetite.

To further investigate how the Fe(II)-induced phase transformation rates of ferrihydrite were affected by the different Me(II), the different phase compositions of the solids during the transformation processes were quantitatively analyzed with the TOPAS program, based on the XRD characterization with CaF_2 as the standard reference. The changes in the relative quantities of ferrihydrite in the reacted solids were obtained (Fig. 2), and a decrease in the relative quantities of ferrihydrite was indicated as the ferrihydrite transformation rate during the Fe(II)-induced transformation of ferrihydrite. The transformation kinetics of the ferrihydrite phase over 4 days (before complete transformation) was fitted using a pseudo-first-order kinetics model (the inserted figure of Fig. 2). The calculated rate constant (k) and the relative coefficient (R) values are listed in Table S1. Ferrihydrite would undergo effective phase transformation when activated by Fe(II) under common conditions (Yang et al., 2010), while the presence of the seven Me(II) were observed to decrease the transformation rates of ferrihydrite (Fig. 2 and Table S1), which were between 0.03 and 1.38 day^{-1}. Comparatively, the k value for Fe(II)-induced ferrihydrite transformation in the absence of Me(II) was 1.47 day^{-1}. All seven Me(II) inhibited ferrihydrite transformation. The relative differences between the observed rate constants were: control (no Me(II)) > Ba > Ca > Mg > Mn > Zn > Ni > Co.

The TEM results for the reacted solids after 60 days also indicated the different degrees of ferrihydrite transformation affected by the different

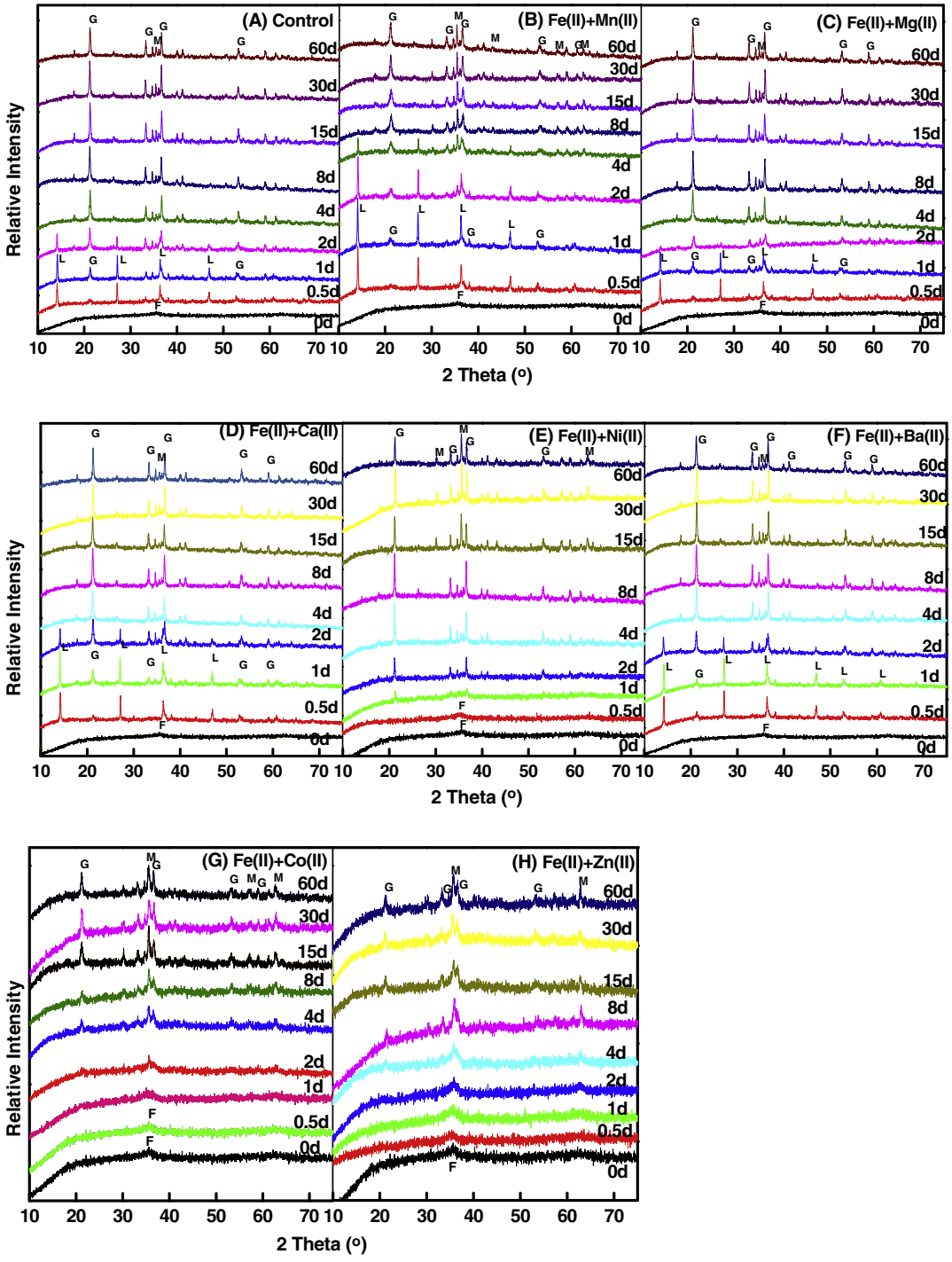

Fig. 1. XRD patterns of the transformed ferrihydrite samples induced by Fe(II) when in the presence of different divalent metal cations. The experiments were carried out at pH 6.5 under anaerobic conditions, with 30 mM of the ferrihydrite, 2.0 mM of the Fe(II) and 1.0 mM of the different Me(II) (Control was the treatment without any Me(II), and the names of the cations represent the treatment with the according cation).

Me(II) (Fig. 3). The "star-shaped" crystalline assemblages of all of the secondary minerals indicated the formation of goethite and magnetite (Hansel et al., 2005; Boland et al., 2014b). When reacted with the alkaline earth metals, i.e., Mg(II), Ca(II), and Ba(II), the dominant composition of the formed secondary minerals was goethite, with a high crystallinity and a relatively decreased value for the full width at half maximum (FWHM) (Wang et al., 2013). The transition Me(II), however, resulted in the formation of more magnetite, along with enhanced crystallinity. From the TEM images, therefore, we observed that the width and length of acicular goethite were larger in the control and the treatments with the supplement of Mg(II), Ca(II),or Ba(II) than those with Mn(II), Co(II), Ni(II), or Zn(II).

3.2. Distribution of Fe(II) species during Fe(II)-induced transformation of ferrihydrite

To explore the affecting mechanisms of Me(II) on Fe(II)-induced ferrihydrite transformation associating with Fe(II), we further investigated the changes of the concentrations of different Fe(II) species during the reactions. Three Fe(II) species, i.e., the dissolved Fe(II) in the filtrate,

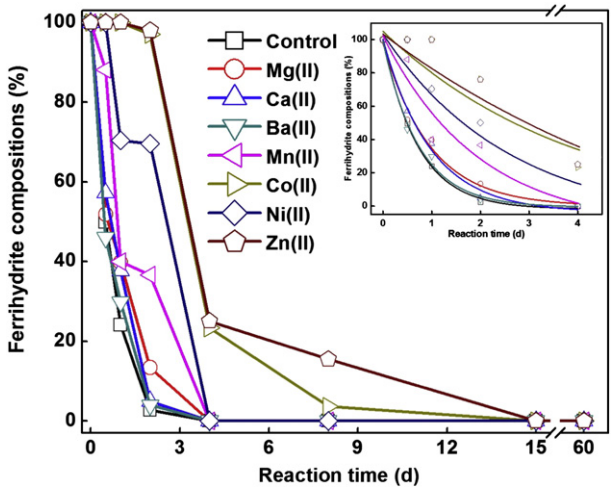

Fig. 2. The changes of ferrihydrite compositions during the Fe(II)-induced phase transformation of ferrihydrite (The inserted figure representing the according pseudo-first-order kinetics model fitting curves of the composition changes). Phase compositions were determined by Rietveld quantitative XRD analysis with using CaF_2 as an internal standard reference. The experimental conditions are the same as that in Fig. 1.

the adsorbed Fe(II) extracted with 0.4 M HCl, and the solid Fe(II) (including the magnetite structural Fe(II)) obtained by dissolving the solids in concentrated HCl, were obtained respectively and their respective concentration changes during the reactions are shown in Fig. 4. The amount of dissolved Fe(II) decreased quickly over 4 days and then remained relatively constant during the Fe(II)-induced transformation of ferrihydrite under different Me(II) treatments (Fig. 4A), whereas the amounts of adsorbed Fe(II) first increased quickly and then decreased gradually (Fig. 4B). The concentrations of solid Fe(II) also increased quickly during the first 5 days and then remained constant at 1.3–1.8 mM across the different Me(II) (Fig. 4C).

The concentration changes of the dissolved Fe(II) in Fig. 4A within 4 days were fitted to a pseudo-first-order kinetics model (Fig. 4D), and the *k* and R values are presented in Table S2. Additional analysis of the relationships between the *k* values of ferrihydrite transformation and the *k* values of the dissolved Fe(II) decrease exhibited a linearly positive relationship (Fig. 5). The results in Fig. 5 indicate that, when with different Me(II), the higher decreasing rates of dissolved Fe(II) may lead to higher transformation rates of ferrihydrite. The largest decrease in rate of the dissolved Fe(II) was obtained with Ba(II) (the Me(II) that minimally inhibited the phase transformation of ferrihydrite, as shown in Table S1). In contrast, the presence of Co(II) or Zn(II), which resulted in much smaller *k* values for the ferrihydrite transformation, led to a less decrease in rates of the dissolved Fe(II) (Fig. 4A) and a higher stabilization ratio of Me(II) in ferrihydrite (Fig. 4C).

4. Discussion

4.1. Effects of different Me(II) on the Fe(II)-induced phase transformation of ferrihydrite

Metal-substituted iron (hydr)oxides have been reported to be more resistant than pure iron (hydr)oxides in the reductive dissolution and Fe(II)-induced transformation (Hansel et al., 2011; Masue-Slowey et al., 2011; Latta et al., 2012b; Massey et al., 2014a). The resistance has been ascribed to the inhibited Fe atom exchange or electron exchange between aqueous Fe(II) and structural Fe(III), in which substituted metals block the reductive dissolution of iron oxides and inhibit bulk electron conduction (Frierdich et al., 2012; Latta et al., 2012b; Neumann et al., 2013). In addition to the above-mentioned factors, environmental factors, such as pH, Fe(II) concentration, temperature, and ionic strength, that affect the Fe(II)-induced phase transformation of iron (hydr)oxides have also been investigated (Hansel et al., 2003, 2005; Das et al., 2010; Boland et al., 2014b). The previous reports suggested that the competitive adsorption of cations with Fe(II) on iron (hydr)oxides (Jones et al., 2009), or the possibly structural substitution of Me(II) (Frierdich and Catalano, 2012) in the iron (hydr)oxide would inhibit Fe(II)-induced phase transformation during the reactions. For ferrihydrite, the competitive adsorption would also influence the Fe(II)-induced phase transformation rates (Ishikawa et al., 2005) and pathway (Hansel et al., 2003; Ishikawa et al., 2004). The competitive adsorption of Me(II) with Fe(II) would be affected by the intrinsic metal properties, such as the binding ability, which further leads to the inhibited Fe(II)-induced phase transformation of ferrihydrite under the controlled constant environmental conditions.

The affinities of cations to iron (hydr)oxides are different due to their binding abilities, which influence the amount of binding of Fe(II) through competitive adsorption/complexation. The concentration changes of different Fe(II) species (Fig. 4) indicate that the added Fe(II) first quickly adsorbed onto the ferrihydrite surface, leading to the decrease of the dissolved Fe(II) and the increase of the adsorbed Fe(II), in which some of the adsorbed Fe(II) was incorporated into the secondary minerals through occlusion or structural incorporation (Jang et al., 2003; Latta et al., 2012b). In line with the Fe(II) incorporation and electron transfer, some of the ferrihydrite was transformed into the secondary minerals with higher crystallinity, i.e., lepidocrocite, goethite, and magnetite (Fig. 1). The solid-associated Fe(II) species (including the adsorbed and incorporated Fe(II)) with iron oxides have been reported to play an important role in the different Fe(II)-catalyzed transformation pathways of ferrihydrite (Boland et al., 2014b).

The main products were goethite when with the Me(II) leading to relatively more amount of adsorbed Fe(II) on ferrihydrite (e.g. control, Mg, Ca, and Ba). When with the Me(II) leading to relatively less amount of adsorbed Fe(II) on ferrihydrite (e.g. Ni, Zn, Co, and Mn), the major products were magnetite and goethite. Hansel et al. (2005) also reported the same results, and they further concluded that the dissolution of produced lepidocrocite and goethite induced magnetite formation with Fe(III)-dependent crystal growth.

To explore the inhibition mechanism with different cations, we investigated the relationships between the binding ability constants (log*K*) (Table S3) of the seven Me(II) (Liu et al., 2014b) and the *k* values of ferrihydrite transformation (Fig. 6A). The results clearly showed that the transformation rates of the ferrihydrite are negatively linearly correlated ($R = 0.95$) with the binding constants of Me(II), indicating the effect of log*K* of the cations on the binding amount of Fe(II) and, consequently, on the transformation rates of the ferrihydrite. In the systems with Me(II) and Fe(II), the log*K* values determined the different existing forms of the cations. In the treatments of Ba(II), Ca(II), Mg(II), and Mn(II), which have a lower log*K* value than Fe(II) (-2.98) (i.e. lower binding abilities than Fe(II)), more Fe(II) was adsorbed and stabilized on the ferrihydrite (Fig. 4), leading to the higher phase transformation rates of ferrihydrite (Fig. 6A). In the treatments of Ni(II) and Zn(II), which have a higher log*K* value than Fe(II), the binding disparity changed accordingly, and less Fe(II) was bound on the ferrihydrite, leading to the lower phase transformation rates of ferrihydrite (Fig. 6A). During the Fe(II)-induced ferrihydrite transformation, the Ba(II), Ca(II), Mg(II), and Mn(II) mainly existed as the dissolved forms, while the Ni(II), Co(II), and Zn(II) were mainly adsorbed and stabilized on the iron oxides (Fig. 7).

At the constant pH condition of 6.5, Me(II) may precipitate as hydrolysis species on the surface of ferrihydrite if the experimental conditions were oversaturated (Ishikawa et al., 2004), especially when reacted with species such as Ni(II), Co(II), and Zn(II) that having higher hydrolysis constants. The probable precipitates at oversaturated conditions would also decrease the contacted Fe(II) with ferrihydrite and result in lower Fe(II)-induced phase transformation rates of ferrihydrite (The hydrolysis constants of the seven cations are provided in Table S4 in

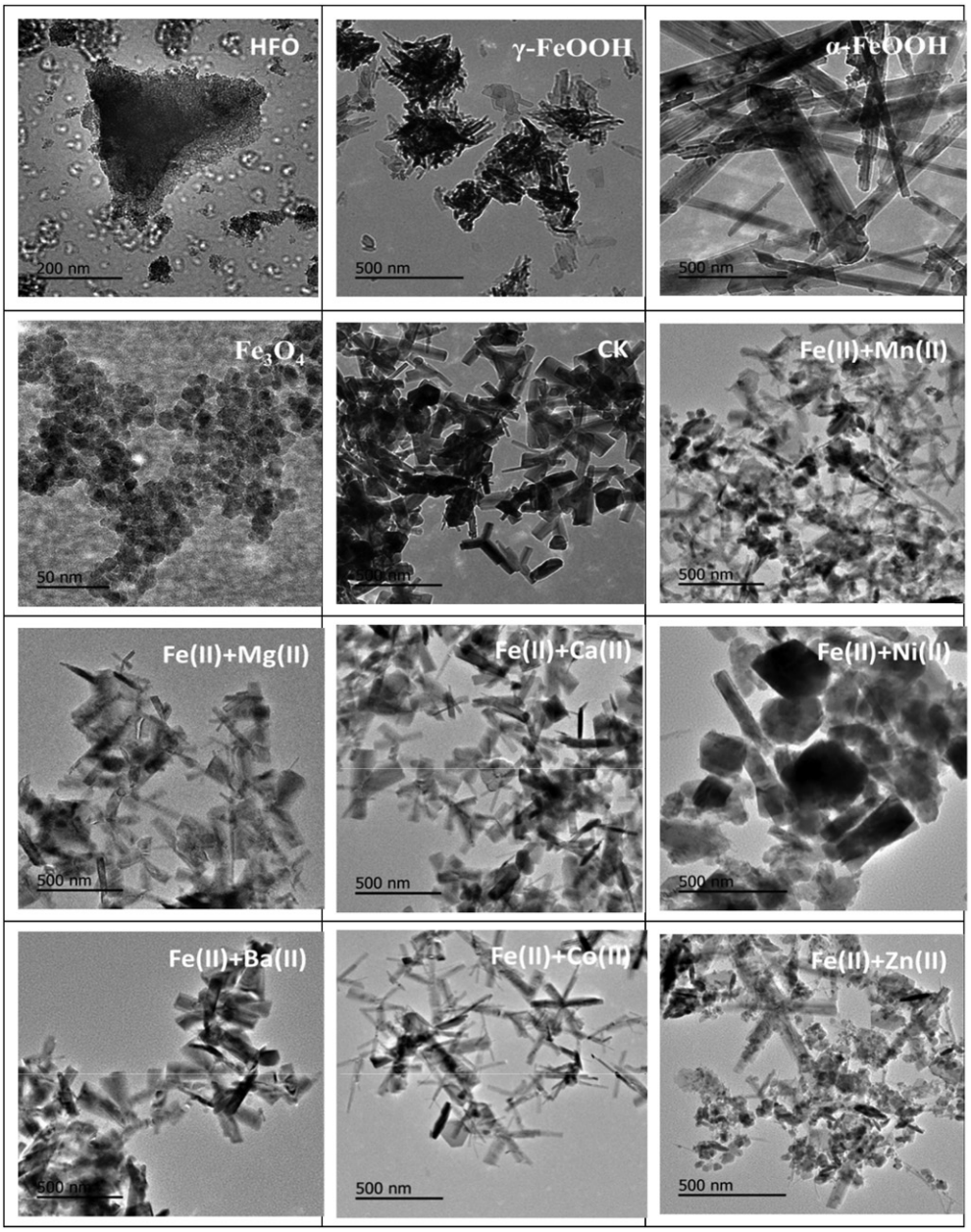

Fig. 3. Transmission electron microscope images of samples after reaction for 60 d during the Fe(II)-catalyzed transformation of ferrihydrite in the presence of different divalent metal cations (γ-FeOOH, α-FeOOH, and Fe_3O_4 were characterized directly after being prepared).

the supplementary materials). However, in the current experimental conditions, the precipitates would not be formed based on the MINTEQ analysis results (data not shown), and thereafter, the competitive sorption of Me(II) with Fe(II) was responsible for the inhibited effects of Fe(II)-catalyzed transformation of ferrihydrite. It is worth noting that Mn(II) was not oxidized during the Fe(II)-induced reaction of ferrihydrite although Mn exists as different oxidation states (2+, 3+, and 4+). In comparison to the control in which Fe(II) was co-existed with ferrihydrite, oxidation states of Mn(III) and Mn(IV) were not detected in the treatment when Mn(II) was mixed with ferrihydrite at the same conditions (data not shown).

Equilibrium speciation analyses of Me(II) and Fe(II) were also carried out using the thermodynamic package Visual MINTEQ 3.0 (Liu et al., 2014b). The information of the calculation were provided in Text S1. The theoretical results (Fig. 8) also indicate that Me(II) with higher log*K* values occupied more surface sites of ferrihydrite and reduced the surface sites for Fe(II) adsorption. With less bound Fe(II), the transformation reactions from Fe(II) in ferrihydrite were weakened and the phase transformation rates of ferrihydrite decreased.

The different Me(II) also affected the anodic peak potentials of ferrous ion on the surface of ferrihydrite. This process in turn changed the phase transformation rates of ferrihydrite. The CV results in Fig. S1 show the positive shifts of the oxidation peak potentials (*E*p) in the Fe(II)-induced transformation systems in the presence of different Me(II) compared with that of the control; a linear relationship between the log*K* and Ep values with different Me(II) was observed (Fig. S2). The *E*p values derived from the CV analyses of the Fe(II)-induced transformation of ferrihydrite in the presence of different Me(II) were negatively correlated with the *k* values of ferrihydrite transformation (Fig. 6B). The oxidation peak potential of a reaction system is affected by various factors, such as pH, ionic strength, the materials of electrode, etc. As to the system of Fe(II)-induced phase transformation of ferrihydrite when with different Me(II), our results indicate the direct relationship between the log *K* values and *E*p values when at the controlled constant

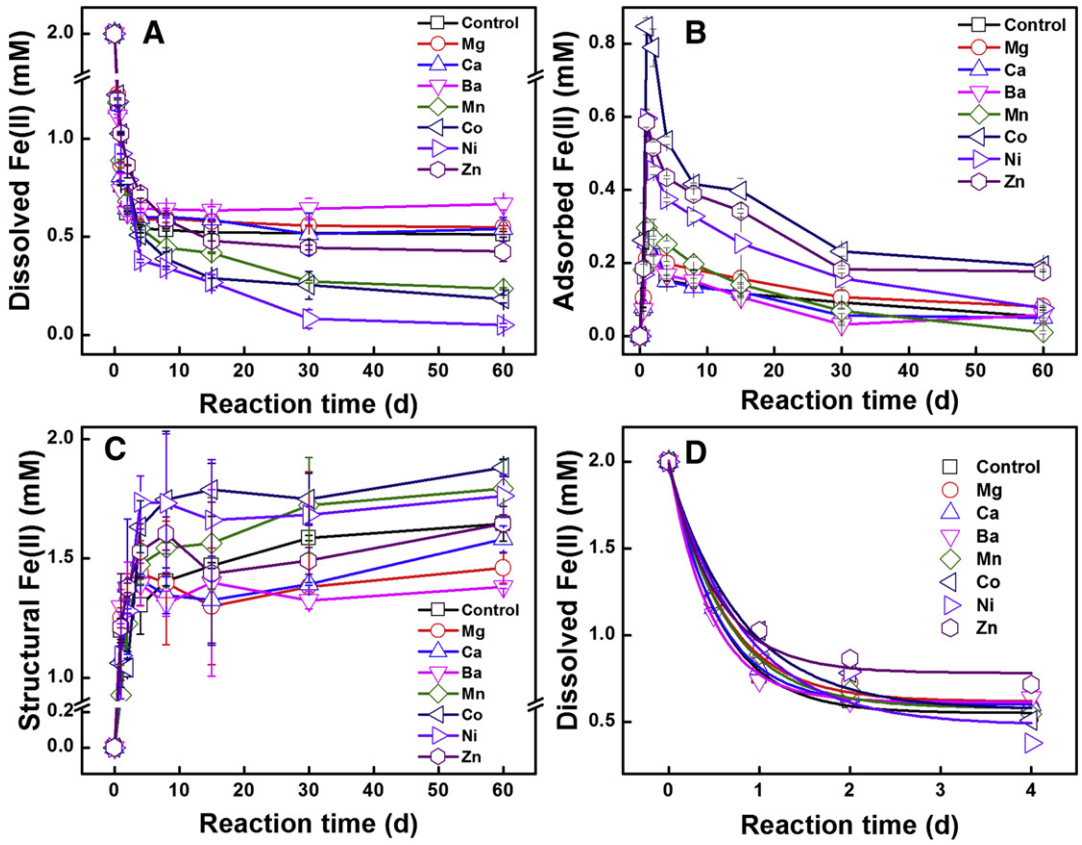

Fig. 4. The concentrations of different Fe(II) species during the Fe(II)-catalyzed transformation of ferrihydrite: (A) dissolved Fe(II), (B) adsorbed Fe(II) (0.4 M HCl extracted), (C) structural Fe(II) (From dissolved solid phase, including Fe(II) of magnetite), and (D) the according pseudo-first-order kinetics model fitting curves of the concentration changes of dissolved Fe(II) in (A).

pH and initial ionic concentrations. This result suggests that the higher binding ability of the Me(II) resulted in the higher oxidation peak oxidation of the system and consequently, led to lower Fe(II)-induced phase transformation rate of ferrihydrite. The decreased oxidation potential of Fe(II) on the ferrihydrite surface resulted in a lower possibility of electron donating, which would consequently decrease the electron transfer efficiency from surface Fe(II) to the bulk ferrihydrite. Therefore, the phase transformation rates of the ferrihydrite decreased as the electron transfer between the surface and bulk of iron oxides has been confirmed to be the main driving force for the Fe(II)-induced phase recrystallization of iron oxides (Yanina and Rosso, 2008; Reddy et al., 2015).

4.2. Stabilization of metal cations during the Fe(II)-induced transformation of ferrihydrite

The Fe(II)-induced recrystallization of iron (hydr)oxides can stabilize the coexisting heavy metals in the structure of the secondary formed iron minerals (Latta et al., 2012a). Previous studies have also reported the formation of metal-incorporated secondary minerals during the Fe(II)-induced transformation of ferrihydrite (Jang et al., 2003; Pedersen et al., 2006; Nico et al., 2009; Boland et al., 2014a; Hoffmann et al., 2014; Massey et al., 2014b). In this study, due to the different properties of Me(II), different amounts

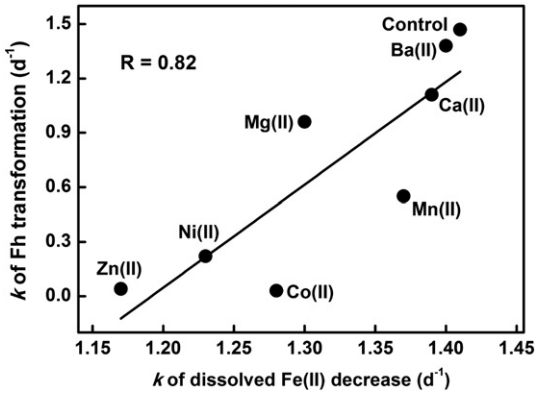

Fig. 5. The relationship between the rates of the Fe(II)-induced transformation of ferrihydrite and the rates of the dissolved Fe(II) decrease with the seven divalent cations.

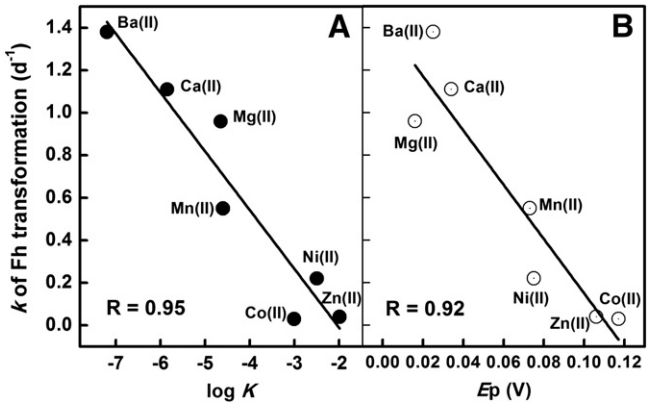

Fig. 6. The relationship between the rates of the Fe(II)-induced transformation of ferrihydrite and (A) binding constants (log*K*) of the seven divalent cations, and (B) the redox potential (*Ep*) of the Fe(II) in the systems.

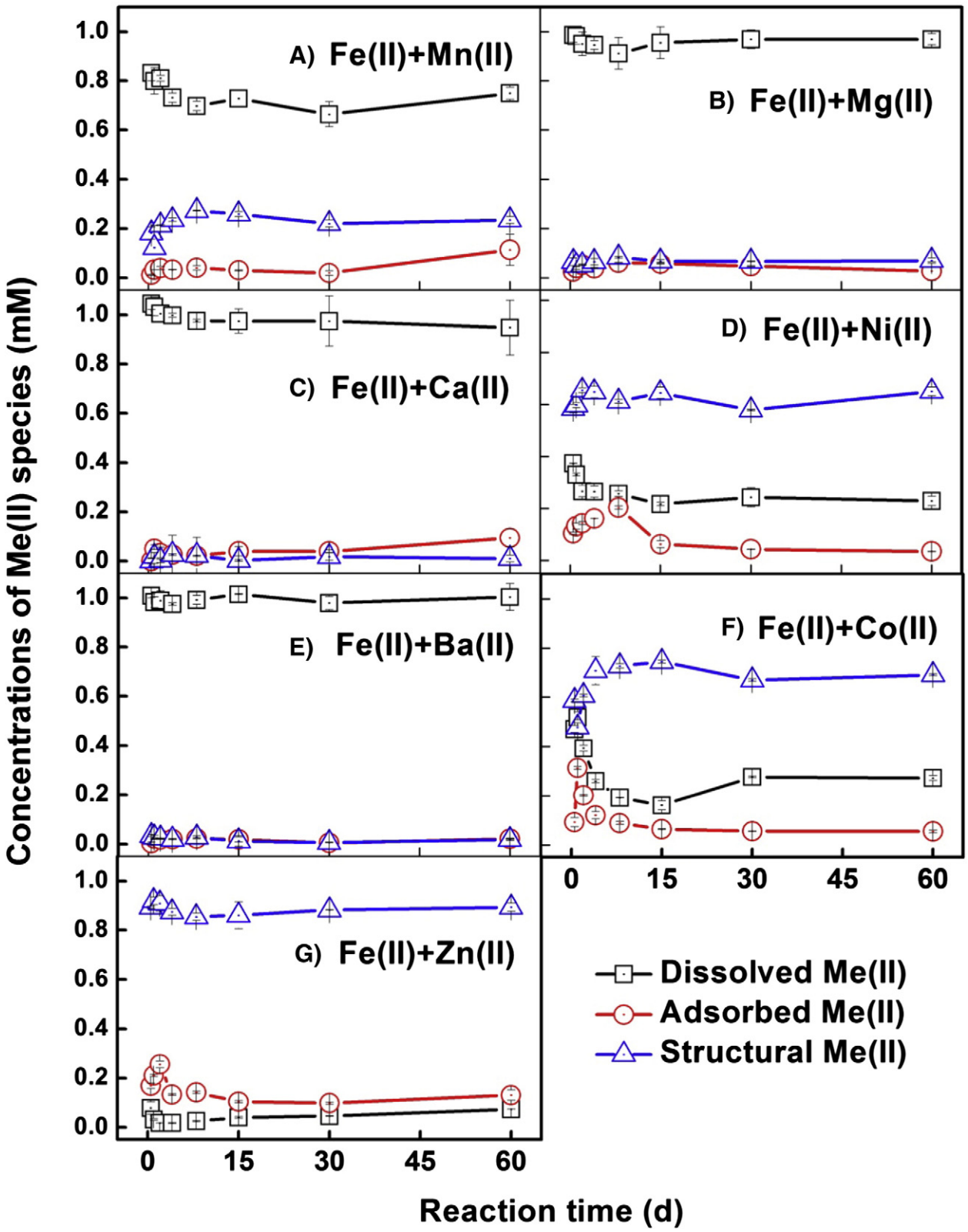

Fig. 7. The concentrations of heavy metal species during the Fe(II)-induced ferrihydrite transformation in the presence of the different cations. Square symbols: dissolved Me(II), circular symbols: adsorbed Me(II) (0.4 M HCl extracted), and triangle symbols: structural Me(II) (From dissolved solid phase).

of cations were stabilized by ferrihydrite or transformed minerals during the Fe(II)-induced transformation of ferrihydrite (Fig. 7). The binding ability of the Me(II) may be one of the important factors that determine the amount of stabilized metals. The transformations involving Me(II) with higher log*K* values, i.e. Ni(II), Co(II), and Zn(II), resulted in larger amounts of stabilized metals in the secondary minerals.

Together with the binding abilities, the other factor such as the possibility of precipitates of the different Me(II) under specific pH condition may also affect the contacted amounts of Me(II), which ultimately affect

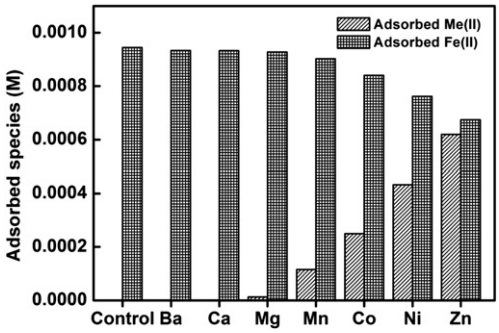

Fig. 8. Calculated concentrations of the adsorbed divalent metal cations and Fe(II) on ferrihydrite during the Fe(II)-catalyzed transformation of ferrihydrite when in the presence of different divalent metal cations, using the thermodynamic package Visual MINTEQ 3.0.

the Fe(II)-induced phase transformation of ferrihydrite and stabilization of Me(II). Additionally, Occlusion and structural incorporation mechanisms were proposed for the metal stabilization (Hansel et al., 2005). However, the specific mechanism responsible for the stabilization of the metals due to the different physicochemical properties of the metals are still needs to be further explored. The study on the effects of different possibilities of different Me(II), such as with MINTEQ modeling, and the exploration of the stabilization mechanisms for different metals, such as with the synchrotron radiation of X-Ray absorption fine structure with the specific metal *K*-edge study, would be important for deep understanding the stabilization mechanism of Me(II) during the Fe(II)-induced phase transformation of ferrihydrite.

5. Conclusions

Iron minerals in soils often coexist with different metal cations, especially in contaminated soils where heavy metals are prevalent. Ferrihydrite, usually with high surface area and low crystallinity, is recognized as an excellent absorbent for stabilization of heavy metals in soils. Our study shows that coexisting divalent metal cations with ferrihydrite can affect the efficiency and pathway of the Fe(II)-induced phase transformation of ferrihydrite significantly. Under the controlled constant conditions (such as the fixed same pH and initial Fe(II) concentrations), the binding abilities of different Me(II) affected the affinity of coexisting Fe(II) to ferrihydrite, which further changed the Fe(II)-induced phase transformation rates and pathways of ferrihydrite. Additionally, this study indicates the stabilization of the metal cations through occlusion/incorporation by the formed secondary iron (hydr)oxides from Fe(II)-induced transformation of ferrihydrite. We expect these findings to bridge the knowledge gap between the contaminated metal cations and the active iron minerals in soils, and also to improve our understanding of the behavior of environmental geochemistry of metal cations in anoxic iron-rich soils.

Acknowledgments

The authors thank Dr. Andrew Frierdich at Monash University for his valuable comments on the manuscript during the preparation. Dr. Michael Massey at California State University, East Bay and one anonymous reviewer are highly appreciated for their valuable comments enhancing the manuscript. This work was funded by the National Natural Science Foundation of China (41420104007 and 41673135), the Guangdong Natural Science Foundation of China (S2013050014266), and One Hundred Talents Programme of the Chinese Academy of Sciences. This research was carried out (in part) at NSRRC in Hsinchu, Taiwan.

Appendix A. Supplementary data

Supplementary data to this article can be found online at http://dx.doi.org/10.1016/j.chemgeo.2016.10.002.

References

Bernasconi, A., Dapiaggi, M., Gualtieri, A.F., 2014. Accuracy in quantitative phase analysis of mixtures with large amorphous contents. The case of zircon-rich sanitary-ware glazes. J. Appl. Crystallogr. 47, 136–145.
Boland, D.D., Collins, R.N., Glover, C.J., Waite, T.D., 2013. An in situ quick-EXAFS and redox potential study of the Fe(II)-catalysed transformation of ferrihydrite. Colloid Surf. A. 435, 2–8.
Boland, D.D., Collins, R.N., Glover, C.J., Payne, T.E., Waite, T.D., 2014a. Reduction of U(VI) by Fe(II) during the Fe(II)-accelerated transformation of ferrihydrite. Environ. Sci. Technol. 48, 9086–9093.
Boland, D.D., Collins, R.N., Miller, C.J., Glover, C.J., Waite, T.D., 2014b. Effect of solution and solid-phase conditions on the Fe(II)-accelerated transformation of ferrihydrite to lepidocrocite and goethite. Environ. Sci. Technol. 48, 5477–5485.
Borch, T, Kretzschmar, R., Kappler, A., Cappellen, P.V., Ginder-Vogel, M., Voegelin, A., Campbell, K., 2009. Biogeochemical redox processes and their impact on contaminant dynamics. Environ. Sci. Technol. 44, 15–23.
Burton, E.D., Bush, R.T., Sullivan, L.A., Mitchell, D.R., 2008. Schwertmannite transformation to goethite via the Fe(II) pathway: reaction rates and implications for iron–sulfide formation. Geochim. Cosmochim. Acta 72, 4551–4564.
Cornell, R.M., Schwertmann, U., 2003. The Iron Oxides: Structure, Properties, Reactions, Occurrences and Uses. 2nd edition. Wiley-VCH GmbH & Co. kGaA.
Dai, C., Hu, Y., 2014. Fe (III) hydroxide nucleation and growth on quartz in the presence of Cu(II), Pb(II), and Cr(III): metal hydrolysis and adsorption. Environ. Sci. Technol. 49, 292–300.
Das, S., Hendry, M.J., Essilfie-Dughan, J., 2010. Transformation of two-line ferrihydrite to goethite and hematite as a function of pH and temperature. Environ. Sci. Technol. 45, 268–275.
Das, S., Hendry, M.J., Essilfie-Dughan, J., 2011. Effects of adsorbed arsenate on the rate of transformation of 2-line ferrihydrite at pH 10. Environ. Sci. Technol. 45, 5557–5563.
De La Torre, A.G., Bruque, S., Aranda, M.A.G., 2001. Rietveld quantitative amorphous content analysis. J. Appl. Crystallogr. 34, 196–202.
Fadrus, H., Malý, J., 1975. Rapid extraction-photometric determination of traces of iron (II) and iron (III) in water with 1, 10-phenanthroline. Anal. Chim. Acta 77, 315–316.
Frierdich, A.J., Catalano, J.G., 2012. Fe(II)-mediated reduction and repartitioning of structurally incorporated Cu, Co, and Mn in iron oxides. Environ. Sci. Technol. 46, 11070–11077.
Frierdich, A.J., Luo, Y., Catalano, J.G., 2011. Trace element cycling through iron oxide minerals during redox-driven dynamic recrystallization. Geology 39, 1083–1086.
Frierdich, A.J., Scherer, M.M., Bachman, J.E., Engelhard, M.H., Rapponotti, B.W., Catalano, J.G., 2012. Inhibition of trace element release during Fe(II)-activated recrystallization of Al-, Cr-, and Sn-substituted goethite and hematite. Environ. Sci. Technol. 46, 10031–10039.
Frierdich, A.J., Helgeson, M., Liu, C.S., Wang, C.M., Rosso, K.M., Scherer, M.M., 2015. Iron atom exchange between hematite and aqueous Fe(II). Environ. Sci. Technol. 49, 8479–8486.
Handler, R.M., Beard, B.L., Johnson, C.M., Scherer, M.M., 2009. Atom exchange between aqueous Fe(II) and goethite: an Fe isotope tracer study. Environ. Sci. Technol. 43, 1102–1107.
Handler, R.M., Frierdich, A.J., Johnson, C.M., Rosso, K.M., Beard, B.L., Wang, C.M., Latta, D.E., Neumann, A., Pasakarnis, T., Premaratne, W.A.P.J., Scherer, M.M., 2014. Fe(II)-catalyzed recrystallization of goethite revisited. Environ. Sci. Technol. 48, 11302–11311.
Hansel, C., Benner, S., Neiss, J., Dohnalkova, A., Kukkadapu, R., Fendorf, S., 2003. Secondary mineralization pathways induced by dissimilatory iron reduction of ferrihydrite under advective flow. Geochim. Cosmochim. Acta 67, 2977–2992.
Hansel, C., Benner, S., Fendorf, S., 2005. Competing Fe(II)-induced mineralization pathways of ferrihydrite. Environ. Sci. Technol. 39, 7147–7153.
Hansel, C., Learman, D., Lentini, C., Ekstrom, E., 2011. Effect of adsorbed and substituted Al on Fe(II)-induced mineralization pathways of ferrihydrite. Geochim. Cosmochim. Acta 75, 4653–4666.
Hoffmann, M., Mikutta, C., Kretzschmar, R., 2014. Arsenite binding to sulfhydryl groups in the absence and presence of ferrihydrite: a model study. Environ. Sci. Technol. 48, 3822–3831.
Ishikawa, T., Minamigawa, M., Kandori, K., Nakayama, T., Tsubota, T., 2004. Influence of metal ions on the transformation of γ-FeOOH into α-FeOOH. J. Electrochem. Soc. 151, B512–B518.
Ishikawa, T., Takeuchi, K., Kandori, K., Nakayama, T., 2005. Transformation of γ-FeOOH to α-FeOOH in acidic solutions containing metal ions. Colloid Surf. A. 266, 155–159.
Jang, J.-H., Dempsey, B.A., Catchen, G.L., Burgos, W.D., 2003. Effects of Zn(II), Cu(II), Mn(II), Fe(II), NO^{3-}, or SO_4^{2-} at pH 6.5 and 8.5 on transformations of hydrous ferric oxide (HFO) as evidenced by Mössbauer spectroscopy. Colloid Surf. A. 221, 55–68.
Jones, A.M., Collins, R.N., Rose, J., Waite, T.D., 2009. The effect of silica and natural organic matter on the Fe(II)-catalysed transformation and reactivity of Fe(III) minerals. Geochim. Cosmochim. Acta 73, 4409–4422.
Larese-Casanova, P., Scherer, M.M., 2007. Fe(II) sorption on hematite: new insights based on spectroscopic measurements. Environ. Sci. Technol. 41, 471–477.
Latta, D.E., Gorski, C., Scherer, M., 2012a. Influence of Fe^{2+}-catalysed iron oxide recrystallization on metal cycling. Biochem. Soc. Trans. 40, 1191–1197.

Latta, D.E., Bachman, J.E., Scherer, M.M., 2012b. Fe electron transfer and atom exchange in goethite: influence of Al-substitution and anion sorption. Environ. Sci. Technol. 46, 10614–10623.
Liu, C.S., Wang, Y.K., Li, F.B., Chen, M.J., Zhai, G.S., Tao, L., Liu, C.P., 2014a. Influence of geochemical properties and land-use types on the microbial reduction of Fe(III) in subtropical soils. Environ. Sci.: Process & Impacts 16, 1938–1947.
Liu, T., Li, X., Waite, T.D., 2014b. Depassivation of aged Fe0 by divalent cations: correlation between contaminant degradation and surface complexation constants. Environ. Sci. Technol. 48, 14564–14571.
Lu, X., Shih, K., Liu, C.S., Wang, F., 2013. Extraction of metallic lead from cathode ray tube (CRT) funnel glass by thermal reduction with metallic iron. Environ. Sci. Technol. 47, 9972–9978.
Massey, M.S., Lezama-Pacheco, J.S., Michel, F.M., Fendorf, S., 2014a. Uranium incorporation into aluminum-substituted ferrihydrite during iron(II)-induced transformation. Environ. Sci. Proc. Impacts 16, 2137–2144.
Massey, M.S., Lezama-Pacheco, J.S., Jones, M.E., Llton, E.S., Cerrato, J.M., Bargar, J.R., Fendorf, S., 2014b. Competing retention pathways of uranium upon reaction with Fe(II). Geochim. Cosmochim. Acta 42, 166–1852.
Masue-Slowey, Y., Loeppert, R.H., Fendorf, S., 2011. Alteration of ferrihydrite reductive dissolution and transformation by adsorbed As and structural Al: Implications for As retention. Geochim. Cosmochim. Acta 75, 870–886.
Michel, F.M., Ehm, L., Antao, S.M., Lee, P.L., Chupas, P.J., Liu, G., Strongin, D.R., Schoonen, M.A.A., Phillips, B.L., Parise, J.B., 2007. The structure of ferrihydrite, a nanocrystalline material. Science 316, 1726–1729.
Neumann, A., Olson, T.L., Scherer, M.M., 2013. Spectroscopic evidence for Fe(II)–Fe(III) electron transfer at clay mineral edge and basal sites. Environ. Sci. Technol. 47, 6969–6977.
Neumann, A., Wu, L.L., Li, W.Q., Beard, B.L., Johnson, C.M., Rosso, K.M., Frierdich, A.J., Scherer, M.M., 2015. Atom exchange between aqueous Fe(II) and structural Fe in clay minerals. Environ. Sci. Technol. 49, 2786–2795.
Nico, P.S., Stewart, B.D., Fendorf, S., 2009. Incorporation of oxidized uranium into Fe (hydr) oxides during Fe(II) catalyzed remineralization. Environ. Sci. Technol. 43, 7391–7396.
Pedersen, H.D., Postma, D., Jakobsen, R., Larsen, O., 2005. Fast transformation of iron oxyhydroxides by the catalytic action of aqueous Fe(II). Geochim. Cosmochim. Acta 69, 3967–3977.
Pedersen, H.D., Postma, D., Jakobsen, R., 2006. Release of arsenic associated with the reduction and transformation of iron oxides. Geochim. Cosmochim. Acta 70, 4116–4129.
Reddy, T.R., Frierdich, A.J., Beard, B.L., Johnson, C.M., 2015. The effect of pH on stable iron isotope exchange and fractionation between aqueous Fe(II) and goethite. Chem. Geol. 397, 118–127.
Rout, K., Mohapatra, M., Anand, S., 2012. 2-line ferrihydrite: synthesis, characterization and its adsorption behaviour for removal of Pb(II), Cd(II), Cu(II) and Zn(II) from aqueous solutions. Dalton Trans. 41, 3302–3312.
Suter, D., Siffert, C., Sulzberger, B., Stumm, W., 1988. Catalytic dissolution of iron(III)(hydr) oxides by oxalic acid in the presence of Fe(II). Naturwissenschaften 75, 571–573.
Toby, B.H., Von Dreele, R.B., 2013. GSAS-II: the genesis of a modern open-source all purpose crystallography software package. J. Appl. Crystallogr. 46, 544–549.
Wang, X., Liu, F., Tan, W., Feng, X., Koopal, L.K., 2013. Transformation of hydroxyl carbonate green rust into crystalline iron (hydr)oxides: influences of reaction conditions and underlying mechanisms. Chem. Geol. 351, 57–65.
Williams, A.G., Scherer, M.M., 2004. Spectroscopic evidence for Fe(II)-Fe(III) electron transfer at the iron oxide-water interface. Environ. Sci. Technol. 38, 4782–4790.
Yang, L., Steefel, C.I., Marcus, M.A., Bargar, J.R., 2010. Kinetics of Fe(II)-catalyzed transformation of 6-line ferrihydrite under anaerobic flow conditions. Environ. Sci. Technol. 44, 5469–5475.
Yanina, S.V., Rosso, K.M., 2008. Linked reactivity at mineral-water interfaces through bulk crystal conduction. Science 320, 218–222.